Purification and characterization of guanylate kinase, a nucleoside monophosphate kinase of *Brugia malayi*

SMITA GUPTA[1], SUNITA YADAV[1], NIDHI SINGH[2], ANITA VERMA[1], IMRAN SIDDIQI[1] *and* JITENDRA K. SAXENA[1]*

[1] *Division of Biochemistry, CSIR-Central Drug Research Institute, Lucknow - 226031, Uttar Pradesh, India*
[2] *Division of Molecular and Structural Biology, CSIR-Central Drug Research Institute, Lucknow - 226031, Uttar Pradesh, India*

(*Received 20 January 2014; revised 21 March 2014; accepted 21 March 2014; first published online 20 May 2014*)

SUMMARY

Guanylate kinase, a nucleoside monophosphate kinase of *Brugia malayi* which is involved in reversible transfer of phosphate groups from ATP to GMP, was cloned, expressed and characterized. The native molecular mass of BmGK was found to be 45 kDa as determined by size exclusion chromatography and glutaraldehyde cross-linking which revealed that the protein is homodimer in nature. This is a unique characteristic among known eukaryotic GKs. GMP and ATP served as the most effective phosphate acceptor and donor, respectively. Recombinant BmGK utilized both GMP and dGMP, as substrates showing K_m values of 30 and 38 μM, respectively. Free Mg^{+2} (un-complexed to ATP) and GTP play a regulatory role in catalysis of BmGK. The enzyme showed higher catalytic efficiency as compared with human GK and showed ternary complex (BmGK-GMP-ATP) formation with sequential substrate binding. The secondary structure of BmGK consisted of 45% α-helices, 18% β-sheets as revealed by CD analysis. Homology modelling and docking with GMP revealed conserved substrate binding residues with slight differences. Differences in kinetic properties and oligomerization of BmGK compared with human GK can provide the way for design of parasite-specific inhibitors.

Key words: *Brugia malayi*, guanylate kinase, nucleoside monophosphate kinase, oligomerization, endproduct inhibition.

INTRODUCTION

Lymphatic filariasis (LF) is a vector-borne disease caused by *Wuchereria bancrofti, Brugia malayi* and *Brugia timori*. Lymphatic filariasis is the second leading cause of permanent and long-term disability with over 40 million infected people suffering from clinical disease manifestation viz. lymphoedema, hydrocoeles and elephantiasis (Bockarie and Deb, 2010). The disease is endemic in 81 countries worldwide with 1·3 billion people at risk and infection of an estimated 120 million people (Crompton, 2010). Currently no vaccine is available for the prevention of LF. There is thus an utmost need to identify new targets for drug development. Current treatment is dependent on existing antifilarials viz. diethylcarbamazine (DEC), ivermectin and albendazole which are highly effective against microfilariae, but exert no effect on adult parasites (WHO, 2010).

Comparative biochemical investigations on the host and parasite are important for establishing potential differences in metabolic activities which can be utilized for selective inhibition of parasite development (Fidock *et al*. 2004). Nucleoside monophosphate (NMP) kinases responsible for the conversion of NMP to nucleotide triphosphates (NTPs) are regarded as potential new chemotherapeutic targets (Kandeel and Kitade, 2011).

Guanylate kinase (GK, ATP: GMP phosphotransferase, guanosine monophosphate kinase, EC 2·7·4·8) belongs to the NMP kinase superfamily. It catalyses the reversible transfer of phosphoryl group from ATP to GMP in the presence of Mg^{+2} (Li *et al*. 1996). Since nucleotide metabolism is a key pathway in the life cycle of any organism, GK plays an important role in guanine nucleotide salvage and metabolic inter-conversion pathways (Oeschger and Bessman, 1966). The enzyme is essential for cGMP recovery and activation of several antiviral drugs viz. acyclovir and ganciclovir (Brady *et al*. 1996). It is considered as a key enzyme for cancer chemotherapy in humans (Miller and Miller, 1980).

Like other NMP kinases, GKs are globular enzymes and consist of CORE, LID and NMP-binding domains (Yan and Tsai, 1999). The enzyme contains parallel β-sheets surrounded by α-helices which constitute the rigid core (CORE domain) of this otherwise flexible protein. The LID domain interacts with ATP when the protein is in the closed conformation. Guanylate kinases, like other NMP kinases, undergo conformational changes from an open and unbound form to a closed form when one ligand (GMP) binds to it and then to a fully closed form when another ligand (ATP) binds to it (Vonrhein *et al*. 1995; Sekulic *et al*. 2002). The closure of the LID and the NMP binding domain

* Corresponding author: Division of Biochemistry Central Drug Research Institute BS10/1, Sector 10, Jankipuram Extension, Sitapur Road, Lucknow - 226031, Uttar Pradesh, India. E-mail: jkscdri@yahoo.com

doi:10.1017/S0031182014000675

onto the core domain assembles the catalytic machinery (Yan and Tsai, 1999). The present paper reports the heterologous expression, purification and characterization of recombinant *B. malayi* guanylate kinase (rBmGK). Studies show that rBmGK follows a sequential mechanism for its catalysis. The significant differences in kinetic properties of host and rBmGK may be utilized for designing inhibitors against human filarial parasites.

MATERIALS AND METHODS

All chemicals were procured from Sigma (St. Louis, USA) unless specifically mentioned. IPTG, Prestained protein ladder, restriction enzyme were purchased from MBI Fermentas (Hanover, MD, USA).

Construction of an expression plasmid for recombinant BmGK

Total RNA of *B. malayi* was extracted by TRIzol® and subjected to cDNA synthesis using cDNA Cycle Kit (Invitrogen, USA). The cDNA was used as a template for BmGK PCR amplification using gene specific primers designed on the basis of sequence available. The forward and reverse primers, with NdeI and XhoI restriction sites (underlined) were 5′ CAT ATG AAG CCT ATT GTA ATA TCA GGT CC 3′ and 5′ CTC GAG TTT CGT CCT TTG AGA CAT AAA TTC 3′, respectively. The resulting 591 bp amplicon was cloned into a pGEMT easy cloning vector. The construct was further subcloned into pET28a expression vector and designated as pET28a-GK. This construct was transformed into *Escherichia coli* BL21 (DE3) cells for protein expression.

Over-expression and purification of recombinant BmGK

Escherichia coli BL21 (DE3) cells harbouring the expression plasmid pET28a-BmGK were cultured at 37 °C in Luria-Bertani (LB) medium containing 50 μg mL^{-1} of kanamycin. When the optical density (OD_{600}) of the culture reached ~0·6, expression of His_6-tagged BmGK was induced by the addition of IPTG at the final concentration of 0·75 mM. The culture was grown at 20 °C for 20 h with shaking at 180 rpm. Cells were then harvested by centrifugation at 8000 ***g*** for 10 min and stored at −20 °C.

The protein purification was carried out by thawing the frozen cells and resuspending them in lysis buffer containing 50 mM NaH_2PO4 (pH 8·0), 300 mM NaCl, 10 mM imidazole and 1 mM PMSF. The bacterial cells were then lysed by sonication (Ultrasonicator). The cell pellet was removed by centrifugation at 8000 ***g*** for 35 min and the supernatant was loaded onto Ni^{+2} -nitrilotriacetic acid (Ni^{+2}-NTA) agarose column pre-equilibrated with lysis buffer. Contaminants were washed with buffer containing 50 mM NaH_2PO4 (pH 8·0), 300 mM NaCl and gradient of imidazole. The bound protein was eluted with buffer containing 50 mM NaH_2PO4 (pH 8·0), 300 mM NaCl, 250 mM imidazole. The specificity of the enzyme was determined by western blotting using anti-His antibody while purity was assessed by 12% SDS-PAGE. The protein concentration was determined by the Bradford method using BSA as a protein standard (Bradford, 1976).

Determination of subunit and native molecular mass

Subunit molecular mass of rBmGK was determined on 12% SDS-PAGE according to the method of Lammelli (Laemmli, 1970). The native molecular mass of rBmGK was estimated by size exclusion chromatography (SEC) using Superose 6/12GR column interfaced with AKTA fast performance liquid chromatography (Amersham). The column was pre-equilibrated with buffer containing 50 mM NaH_2PO_4 and 100 mM NaCl (pH 8·0) with the flow rate of 0·40 mL min^{-1}. The column was calibrated with standard molecular weight markers viz. chymotrypsinogen (25 kDa), ovalbumin (45 kDa), bovine serum albumin (66 kDa) and catalase (232 kDa). The native molecular mass of rBmGK was determined by plotting the logarithmic of molecular weight of standard molecular markers with their respective elution volume observed by SEC. The native molecular mass of rBmGK in reducing environment was determined by adding 5 mM β-mercaptoethanol (βME) in all buffers. Glutaraldehyde cross-linking was done as reported previously (Singh *et al*. 2008) and the molecular mass of cross-linked BmGK was determined on 10% SDS-PAGE.

Generation of polyclonal antibodies and western immunoblotting

Purified recombinant protein (150 μg) was emulsified in Freund's complete adjuvant and injected subcutaneously in a rabbit. After 4 weeks, a booster dose of 150 μg of purified BmGK emulsified in Freund's incomplete adjuvant was injected and blood was collected after 10 days following this booster dose. Antibody titre was measured by ELISA (Sambrook *et al*. 1989). For studying expression of BmGK in different life stages of *B. malayi*, western immunoblotting was performed. Purified BmGK as well as lysate of L3, adults and microfilariae (mf) of *B. malayi*, were resolved on 12% SDS-PAGE. The resolved proteins were electro-blotted on nitrocellulose membrane and blocked overnight at 4 °C with 5% skimmed milk in PBS. The membrane was

https://doi.org/10.1017/S0031182014000675 Published online by Cambridge University Press

incubated with anti-BmGK serum at a dilution 1 : 1000 followed by secondary antibody anti-rabbit IgG coupled with horseradish peroxidase at dilution of 1 : 1000 in blocking buffer (5% skimmed milk in PBS) for 3 h at room temperature. Finally, blot was developed using diaminobenzidine (DAB) as substrate.

Activity assay and kinetics

The BmGK activity was determined using a coupled spectrophotometric assay with pyruvate kinase and lactate dehydrogenase (Agarwal *et al*. 1978). The reaction medium (final volume 1 mL) contained 50 mM Tris/HCl pH 7·5, 50 mM KCl, 1 mM $MgCl_2$, 1 mM phosphoenol pyruvate (PEP), 0·5 mM ATP, 0·05 mM GMP, 0·05 mM NADH, 2 units lactate dehydrogenase and 1 unit pyruvate kinase. The decrease in absorbance at 340 nm was monitored by adding 10 μg BmGK at 25 °C in UV-Vis 2450 (Shimadzu, Japan) spectrophotometer. One unit of enzyme is defined as that amount of enzyme catalysing the production of 1 μmol GDP per min at 25 °C.

In order to determine the reaction mechanism of BmGK catalysis, a Lineweaver Burk graph was plotted by varying GMP concentrations (0·01–0·5 mM) and ATP concentrations (0·1, 0·2, 0·5 and 1·0 mM). Different phosphate acceptors GMP, dGMP, dCMP, CMP, IMP, XMP, AMP, dAMP, UMP, dTMP as well as different phosphate donors ATP, dATP, GTP, UTP, CTP, TTP were tested for BmGK activity. Various metal ions (Mg^{+2}, Mn^{+2}, Zn^{+2}, Ca^{+2}, Ni^{+2}) were tested for their effect on recombinant BmGK. GTP and Mg^{+2} were tested at different concentration to study their regulatory effect. Effect of reducing agents [Dithiothreitol (DTT) and βME] and different group-specific reagents viz. ethylenediaminetetraacetic acid (EDTA), p-chloromercuribenzoate (pCMB) and N-ethylmaleimide (NEM) was studied by incubating with enzyme in buffer for 10 min. Diethyl pyrocarbonate (DEPC) and phenylmethylsulfonyl fluoride (PMSF) effect was studied by incubating the enzyme in phosphate buffer (pH 6·0) for 30 min. The inhibitory effect of antifilarials and antihelminthic compounds viz. DEC, ivermectin, suramin, aurin and levamisole was tested by incubation for 10 min with rBmGK. Ivermectin was dissolved in DMSO and an equal amount of DMSO was added to control and activity was measured.

Effect of temperature and pH on reaction catalysis

Effect of temperature on the activity of rBmGK was observed by measuring the enzyme activity at various temperatures after incubation of 10 min. Activation energy of the reaction was calculated from the slope ($-E_a/R$) of the Arrhenius plot [$k = A.e - E_a/RT$; $\ln k = \ln A - (E_a/RT)$], where A represents the Arrhenius constant, E_a is the activation energy, R is the gas constant ($8{\cdot}314\ Jmol^{-1}\ K^{-1}$) and T is the absolute temperature in °K (Maenpuen *et al*. 2009). For the optimal pH determination, enzyme activity was determined using different pH viz., sodium phosphate buffer (pH 6·0–7·0), Tris-HCl buffer (pH 7·5–8·5) and glycine–NaOH (pH 9·0–10·0).

Spectroscopy

Fluorescence spectra were recorded in Perkin Elmer LS50b luminescence spectrometer at 25 °C in a 5 mm path-length quartz cell. BmGK concentration was 5 μM while concentration of GTP was (0–2·0) mM. For monitoring intrinsic tryptophan fluorescence, the excitation wavelength of 290 nm was used and the spectra were recorded between 300 and 400 nm.

CD spectrum was recorded with Jasco J810 CD polarimeter (JASCO, Japan) between 190 and 250 nm using a cuvette of 1·0 cm path length. A scanning with buffer without protein was recorded under identical conditions to determine the background spectra. 5 μM BmGK in 50 mM phosphate buffer pH 7·0 was used for CD spectra and the data were analysed by using K2D2 software (Andrade *et al*. 1993).

Homology modelling and docking study of BmGK

A homology model was constructed to explore the 3D structure of BmGK and to study its structure–function relationship. BlastP of BmGK sequence (Bm1_09150) against PDB was performed to find a suitable template. 1EX7, crystal structure of yeast guanylate kinase in complex with guanosine-5′-monophosphate was selected as a template showing 48% homology. A model was generated using Modeller 9v10 programme (Sali and Blundell, 1993). The modelled structure of BmGK was superimposed on the template and this model was then subjected to SAVeS server (http://nihserver.mbi.ucla.edu/SAVES/) for structural validation.

To study the possible binding mode and interaction pattern Surflex-Dock was employed. It uses an empirical scoring function and a patented search engine to dock ligands into a protein's binding site (Jain, 2003). The mode of interaction of the ligand GMP in the crystal structure against (1EX7) PDB was used as a reference. Amber7FF99 charges were assigned for the protein and side chain amides and bumps were fixed. The maximum number of poses was set to 20 and no constraints were used to perform molecular docking. Ligand (GMP) was prepared with surflex for searching mode. The prepared protein was docked with GeomX mode.

https://doi.org/10.1017/S0031182014000675 Published online by Cambridge University Press

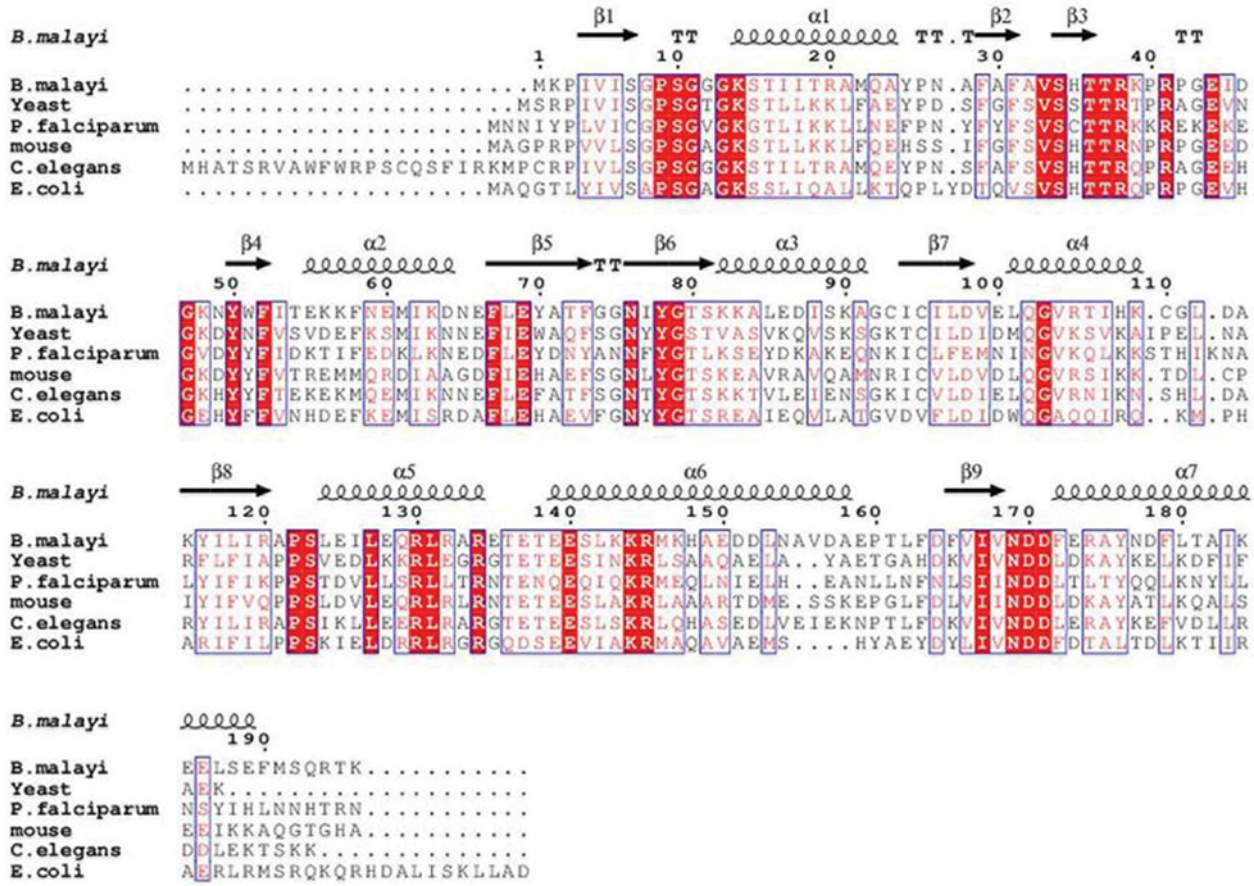

Fig. 1. Amino acid sequence alignment of Guanylate kinases of *B. malayi*, yeast, *P. falciparum*, mouse, *C. elegans* and *E. coli*. Amino acid sequences were retrieved from KEGG and alignments were performed with Clustal W and ESPript 2·2 web tool. The characteristic secondary structure α helices and β sheets are indicated above the sequence. Invariant residues are highlighted as shaded boxes.

RESULTS

Sequence analysis and phylogenetic comparison

Sequences of GKs from different organisms were retrieved from KEGG (http://www.genome.jp/kegg/) and the sequences showing high homology in BLAST analysis (blast.ncbi.nlm.nih.gov/) were aligned by ClustalW (http://www.genome.jp/tools/clustalw/) and ESPript 2·2 web tool (http://espript.ibcp.fr/ESPript/ESPript/) (Fig. 1). The sequence comparison of GKs from *Caenorhabditis elegans*, humans, *Saccharomyces cerevisiae, E. coli* and *Plasmodium falciparum* revealed 30–60% amino acid conservation. The sequence of BmGK showed three regions: CORE, LID and NMP-binding domains (GMP binding). The glycine-rich motif (also called a P-loop) present at the N terminus of different GKs was found to be conserved in *B. malayi*. The α-3 helix, which has a critical role in domain movement and substrate recognition, is amphipathic in mouse, humans, *E. coli* and yeast with conserved Val residues while it did not show similar conservation in BmGK. Evolutionary relationships of GKs with the aligned sequences are shown in the phylogenetic tree (Fig. 2) constructed using the MEGA5 program. The clustering indicated that BmGK is closely related to *C. elegans* and humans but distantly related to *P. falciparum*.

Construction of an expression plasmid, over-expression and purification of rBmGK

The BmGK gene was PCR amplified and cloned into a pET28a vector. The rBmGK was over-expressed in BL21 (DE3) *E. coli* cells by induction with IPTG and the soluble protein was purified by Ni-NTA affinity chromatography. The yield of purified rBmGK was found to be 15 mg L^{-1} of culture. The presence of a single band after western blotting using a penta-His antibody revealed specificity of the purified protein (Fig. 3B) while its subunit molecular mass as determined by 12% SDS PAGE was found to be ~25 kDa (Fig. 3A), consistent with the size estimated from the amino acid sequence of BmGK including both N and C terminus His tag.

Native molecular mass determination

The molecular weight of rBmGK was found to be 45 kDa, which suggests that rBmGK is a homodimeric protein (Fig. 3C). The glutaraldehyde

https://doi.org/10.1017/S0031182014000675 Published online by Cambridge University Press

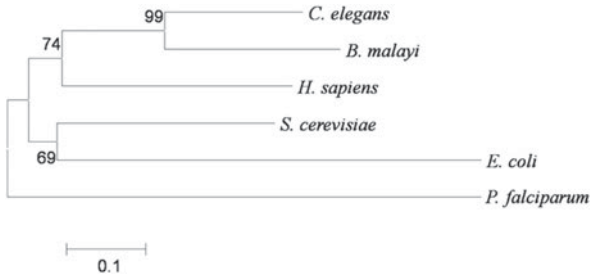

Fig. 2. A molecular phylogenetic tree of BmGK generated by the neighbour-joining (NJ) method using MEGA5 software. An unrooted phylogenetic tree was generated based on the alignment of the amino acid sequences of *C. elegans, B. malayi, H. sapiens, S. cerevisiae, P. falciparum* and *E. coli*. The scale bar indicates an evolutionary distance of amino acid substitutions per position.

cross-linking experiment also showed two cross-linked products on 10% SDS-PAGE corresponding to monomer and dimer position (Fig. 3D). The dimeric nature of the protein was further confirmed by native PAGE (data not shown). rBmGK purified in a reducing environment containing βME also eluted at a position similar to the dimeric form (Supplementary Fig. S1). Thus the dimeric nature of BmGK was confirmed in native as well as in reducing conditions.

Western immunoblotting to study expression of recombinant BmGK in parasite

Polyclonal antibodies raised in rabbit using rBmGK showed a titre value of 1 : 250 000. The results of the western blot demonstrated that anti BmGK antibodies raised in rabbit specifically recognized rBmGK as well as L3, adult and microfilariae (mf) stages of *B. malayi* (Fig. 3E).

Kinetic study of rBmGK

rBmGK activity was measured by using pyruvate kinase-lactate dehydrogenase coupled assay. K_m values for GMP and dGMP were found to be 30 and 38 μM, respectively (Supplementary Fig. S2A & B). The kinetic properties of the protein are shown in Table 1. The double reciprocal plot at different concentrations of GMP with different ATP concentrations showed a series of converging lines (Fig. 4C). The observed intersecting pattern of straight lines indicated a sequential mechanism for BmGK catalysis. GMP was the preferred phosphate acceptor as compared with dGMP, AMP and dAMP. Among different NTPs examined, ATP was found to be the most effective phosphate donor followed by dATP and GTP (Table 2). GTP acts as a phosphate donor (20%) for BmGK, but when used as a ligand at higher concentrations, it was inhibitory to the enzyme (Fig. 5A). The binding of GTP to BmGK was also observed by quenching of its intrinsic fluorescence intensity. The intrinsic fluorescence spectrum of native BmGK was quenched in the presence of increasing concentration of GTP (Fig. 5). Based on the quenching data, K_d value calculated for the binding of GTP to BmGK was found to be 1×10^{-3} M^{-1} (data not shown).

Since PK utilizes Mg^{+2} as a cofactor, concentration of PK in each reaction is at least two orders of magnitudes lower than the lowest Mg^{+2} concentration used (Tan *et al*. 2009). Therefore, PK should have a negligible effect on the reaction. Different concentrations of Mg^{+2} were tested and it was observed that increasing free Mg^{+2} (un-complexed with ATP) enhanced BmGK activity at fixed ATP concentration (Fig. 4D). Different combinations of metal ions with Mg^{+2} were tested but activity was detected only with Mn^{+2} while Zn^{+2}, Ca^{+2}, Ni^{+2} inhibited the enzyme activity drastically. EDTA at 1 mM inhibited 100% BmGK activity indicating that divalent metal ions are required for activity. Sulphydryl group inhibitors (pCMB and NEM), reducing agents (DTT and BME) and His modification by DEPC did not cause any change in activity of rBmGK while PMSF at 5 mM inhibited BmGK activity (Table 3). Among the known antifilarials and antiparasitic compounds tested for inhibition of rBmGK activity, suramin and aurin showed 83·5 and 82% inhibition at 10 and 50 μM, respectively while DEC, ivermectin and levamisole did bring inhibition but at higher concentrations (Table 4). DMSO used in solubilization of ivermectin did not show any effect on rBmGK activity.

Effect of temperature and pH on BmGK activity

The catalytic activity of rBmGK measured at different temperatures showed an increased rate constant as temperature was increased to 37 °C and decreased above it (Fig. 4B). The optimum temperature for the reaction was found to be 37 °C. An Arrhenius plot between logarithm of activity and reciprocal of absolute temperature was linear over the range of 15–40 °C with activation energy of reaction 28·6 kJ mol^{-1} (inset Fig. 4B). Similarly, effect of different pH was measured and it was found that pH 7·5 was the optimum pH for the catalytic reaction and activity diminished above and below it (Fig. 4A).

Secondary structure determination by CD

BmGK showed a typical α/β type secondary structure composition as observed by the far-UV CD spectrum of the protein (Fig. 6). BmGK is composed of 45% α-helices, 18% β-sheets and rest is assumed to be a random coiled structure. The result supports the homology model prediction for secondary structure composition.

https://doi.org/10.1017/S0031182014000675 Published online by Cambridge University Press

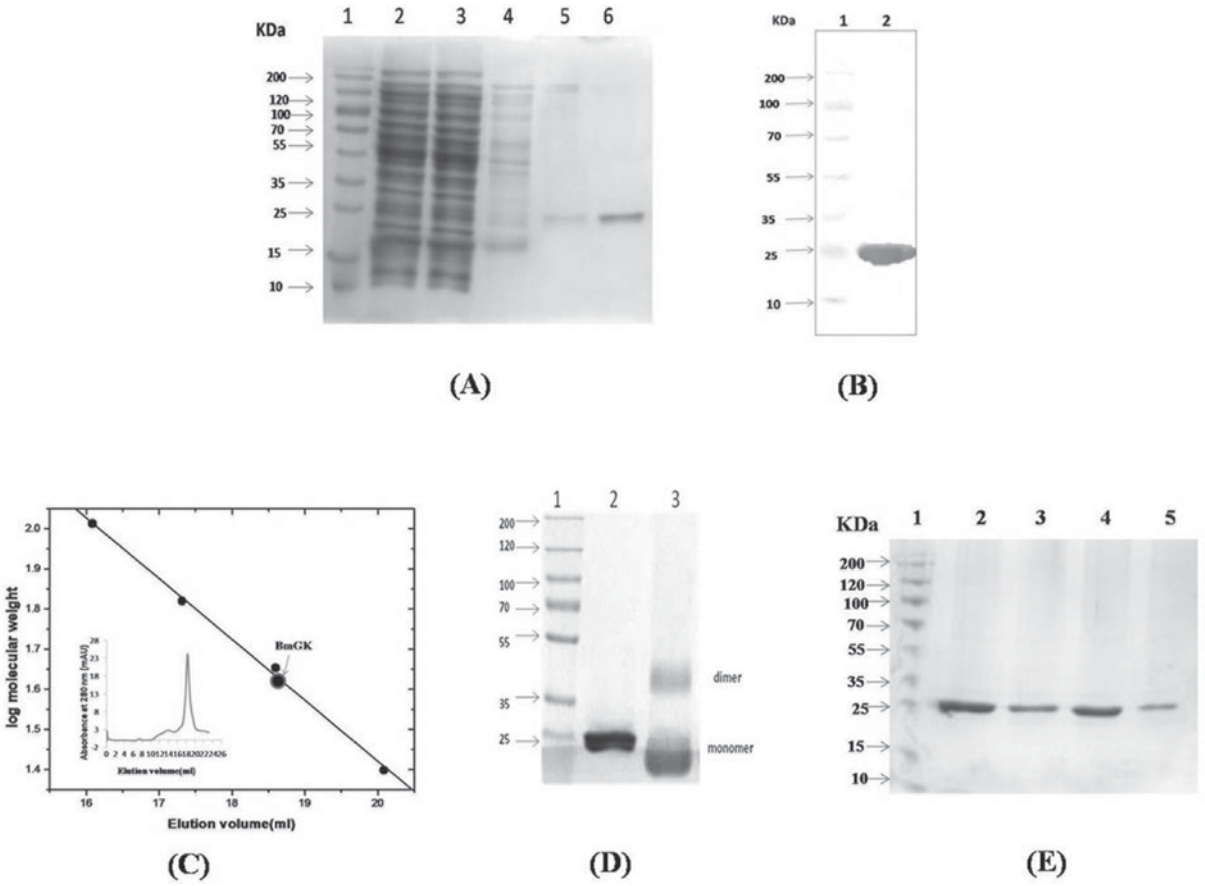

Fig. 3. Purification and characterization of BmGK. (A) 12% SDS-PAGE of purified recombinant BmGK. Lane 1 – Prestained protein ladder, Lane 2 – Sonicated supernatant, Lane 3 – Flowthrough after Ni-NTA column, Lanes 4 & 5 – Washing of Ni-NTA column, Lane 6 – Eluted protein (250 mM imidazole) from Ni-NTA affinity column; (B) Western blotting using penta His antibody: Lane 1 – Prestained Protein ladder, Lane 2 – Purified recombinant BmGK protein; (C) Determination of native molecular mass of BmGK: Logarithmic plot of elution volumes *vs* molecular weights. The native molecular mass of the protein was determined by FPLC using Superose 6/12 gel filtration column. The following proteins were used as standard: chymotrypsinogen (25 kDa) ovalbumin (45 kDa), bovine serum albumin (66 kDa) and catalase (232 kDa). Inset shows Size Exclusion Chromatography profile of BmGK; (D) 10% SDS-PAGE showing glutaraldehyde cross linked BmGK: Lane 1 – Prestained protein ladder, Lane 2 – Recombinant BmGK, Lane 3 – Cross-linked BmGK; (E) Western immunoblotting using anti- BmGK serum for detection of BmGK in different life stages of *B. malayi*: Lane 1 – Prestained protein ladder, Lane 2 – Purified recombinant BmGK protein, Lane 3 – L3 *B. malayi* extract, Lane 4 – Adult *B. malayi* extract , Lane 5 – Microfilariae (mf) *B. malayi* extract.

Homology modelling and docking with GMP

Structural superimposition with the yeast template showed root mean square difference (RMSD) of 0·247 Å. Both have identical folding and it consists of 7 alpha helices and 9 beta sheets connected by turn(s)/loop(s) (Fig. 7A). Docking studies carried out with the BmGK model showed 94·9, 4·0, 1·1 and 0·0% residues in core, allowed, generously allowed and disallowed region, respectively in Ramachandran plot (Supplementary Fig. S3).

A docking study of GK produced a conformation close to co-crystallized conformation of template, suggesting a conserved binding mode of the substrate (GMP) (Fig. 7B). The docking complex assumed to represent ligand–receptor interactions was selected based on three criteria: (i) docking score of the pose possessing the highest docking score, (ii) orientation of the ligand into the active site in a similar manner with the co-crystallized ligands orientation and (iii) the preservation of key interactions. Ser34, Glu69 and Glu100 showed possible hydrogen bonding with a guanosine ring. Arg38, Tyr78 and Arg41 were found to be involved in hydrogen bonding with phosphate moiety of GMP (Fig. 7C). These bonds are synchronous with the template in consideration. In order to study the hydrophobic interactions of GMP, the hydrophobic residues within 5 Å range were considered. This included Val99, Phe73, Tyr78, Tyr70, Ala71, Gly103, Tyr50, Thr80 and Gly79.

DISCUSSION

The availability of *B. malayi* genome has provided sequences to identify new drug targets. The enzyme was selected based on essentiality of GK in *B. malayi*. GK plays an important role in nucleotide metabolism

https://doi.org/10.1017/S0031182014000675 Published online by Cambridge University Press

Table 1. Comparative kinetic parameters of recombinant BmGK and other organisms

Properties	*B. malayi*[a]	*P. falciparum*[b]	Yeast[c]	Humans[d]	Mouse[e]	*A. thalliana*[f]	*E. coli*[g]
Sub-unit mass (kDa)	~ 24	24	21	21·6	21·9	42·7	~ 21
Oligomerization	Dimer	Monomer	Monomer	Monomer	Monomer	Monomer	Dimer/tetramer[h]
K_m^{GMP} (μM)	30	22·4	91	50	25	105	ND
K_{cat} (s^{-1})	1500	946	394	500	426	97	ND
K_{cat}/K_m(s^{-1} M^{-1})	$5{\cdot}0\times10^7$	$4{\cdot}2\times10^7$	$0{\cdot}432\times10^7$	1×10^7	$1{\cdot}7\times10^7$	$0{\cdot}092\times10^7$	ND
K_m^{dGMP} (μM)	38	74·6	ND	35	ND	ND	30
K_{cat}(s^{-1})	510	43	ND	200	ND	ND	ND
K_{cat}/K_m(s^{-1} M^{-1})	$1{\cdot}34\times10^7$	$5{\cdot}8\times10^7$	ND	6×10^6	ND	ND	ND

ND, Not detected.
[a] Present study.
[b] Kandeel *et al.* (2008).
[c] Li *et al.* (1996).
[d] Auvynet *et al.* (2009).
[e] Willmon *et al.* (2006).
[f] Kumar *et al.* (2001).
[g] Oeschger and Bessman (1966).
[h] Gentry *et al.* (1993).

since it is involved in DNA and RNA biosynthesis and provides precursors to various metabolic pathways (Oeschger and Bessman, 1966). GK is one of the key targets in cancer chemotherapy as it is involved in activation of several pro-drugs (Sekulic *et al.* 2002). Hence its role in filarial parasite metabolism has been studied by successful cloning, expression and biochemical characterization. Molecular modelling and docking with GMP was carried out to understand its structure-activity relationship.

Guanylate kinases show low primary structure identity, yet they share a similar fold, which consists of three structurally distinct regions viz. CORE, LID and NMP-binding regions. Besides the similar fold there is an important difference between prokaryotic and eukaryotic GK. The eukaryotic enzymes are monomers while prokaryotic GK are oligomers (dimers, tetramers or hexamers) (Gentry *et al.* 1993; Hible *et al.* 2005, 2006*a*; Eftimie *et al.* 2007). The native molecular mass of rBmGK suggested a dimeric form of enzyme. The result is supported by glutaraldehyde cross-linking and showed similarity in cross-linking pattern to *E. coli* GK (Hible *et al.* 2005, 2006*a*). Furthermore, the similar elution profile of rBmGK in the presence and absence of a reducing agent, β-mercaptoethanol, ruled out the possibility of disulphide-mediated dimer and further supplemented our observation. However, the C terminal extension is absent in the BmGK sequence, which is considered a critical determinant of basic dimeric folding unit in prokaryotic GKs with dimeric/hexameric structure (Hible *et al.* 2005, 2006*a*). It is noteworthy that previous structural studies of eukaryotic GKs did not reveal a dimeric form as observed in rBmGK, which distinguishes the enzyme from its eukaryotic counterpart host, humans. Thus, the dimeric structure of the protein seems to provide an adequate active site conformation in which electrostatic interactions may play a dominant role.

Biochemical characterization of enzyme revealed that rBmGK is sensitive to change in pH and temperature with activation energy estimated to be of the same order of magnitude to that of muscle cytosolic adenylate kinase (Zhang *et al.* 1993). While BmGK K_m for dGMP was found to be similar to humans (Auvynet *et al.* 2009), differences were found with K_m of GMP as compared with humans, mouse, yeast, *P. falciparum* and *Arabidopsis thaliana* (Li *et al.* 1996; Kumar *et al.* 2001; Willmon *et al.* 2006; Kandeel *et al.* 2008; Auvynet *et al.* 2009). Lower K_m value for GMP as compared with the human enzyme indicates a higher affinity for GMP and thus a tendency to convert substrate into product at a higher rate. The catalytic efficiency (K_{cat}/K_m) of GK was also found to be higher for *B. malayi* as compared with human GK. Higher catalytic activity of the parasitic enzyme may be due to greater requirement of nucleotides for rapid multiplication. The observed converging pattern of intersecting

https://doi.org/10.1017/S0031182014000675 Published online by Cambridge University Press

Table 2. Nucleotide specificity of rBmGK

Nucleotides (Phosphate acceptors)	Relative activity (%)	Nucleotides (Phosphate donors)	Relative activity (%)
GMP	100	ATP	100
dGMP	74	dATP	30
AMP, dAMP	31	GTP	20
dTMP ,UMP	0	CTP	0
CMP, dCMP	0	UTP	0
IMP, XMP	0	TTP	0

Experiments were performed at 25 °C at pH 7·5. Activities are expressed as percentage in comparison with a control using ATP and GMP as substrates. The concentration of each nucleotide added to the reaction was 0·05 mM for phosphate acceptors and 0·5 mM for phosphate donors.

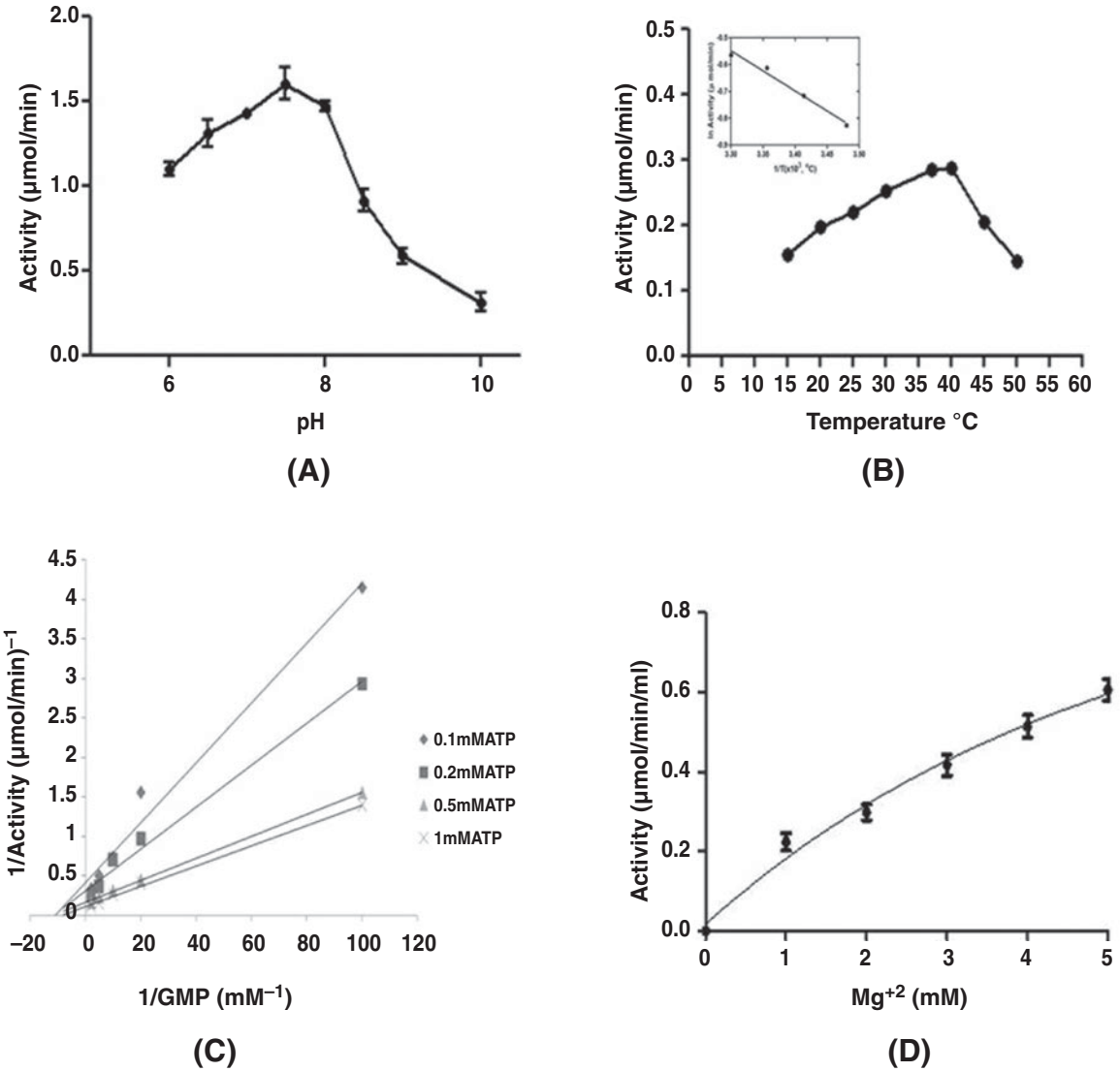

Fig. 4. Effect of pH, temperature and Mg^{+2} on activity of BmGK and its reaction mechanism. (A) Activity was measured using buffers of different pH as described in Materials and Methods; (B) Effect of temperature: The enzyme activity was measured at different temperature as described in Materials and Methods. Inset shows the Arrhenius plot of ln Activity *vs* the reciprocal of absolute temperature for calculation of activation energy; (C) Lineweaver Burk plot at different concentrations of GMP (0·01–0·5 mM) and ATP (0·1, 0·2, 0·5 & 1·0 mM): The activity was measured as described in Materials and Methods; (D) Effect of different concentration of Mg^{+2} on activity of BmGK.

https://doi.org/10.1017/S0031182014000675 Published online by Cambridge University Press

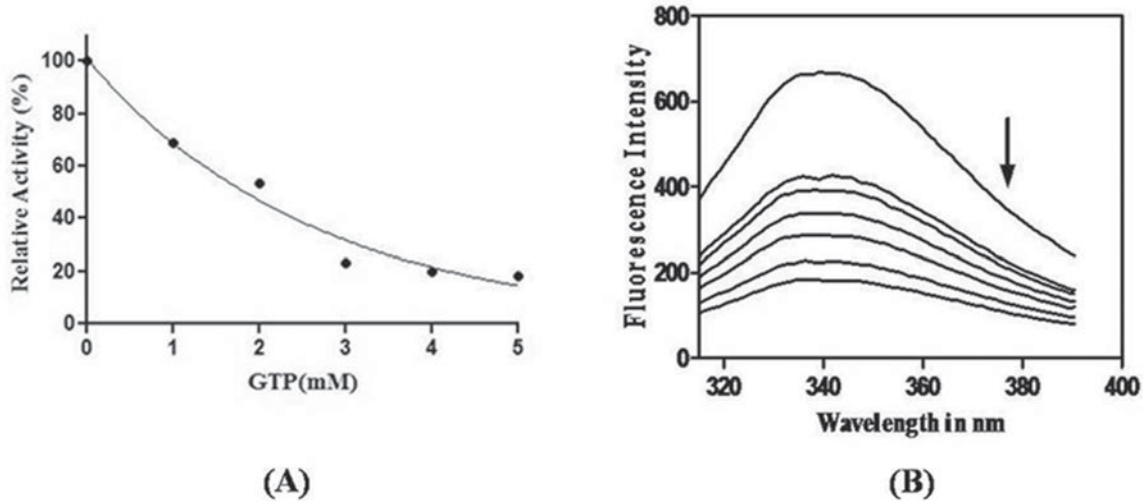

Fig. 5. Effect of GTP on activity and intrinsic fluorescence of BmGK. (A) Enzyme was incubated with increasing concentration of GTP for 10 min and activity was measured as described in 'Materials and Methods'; (B) Intrinsic fluorescence spectra of BmGK in presence of GTP. Arrow indicates increasing concentration of GTP in the range (0–2·0) mM Fluorescence spectra were recorded upon excitation at 290 nm and emission between 300–400 nm.

Table 3. Effect of group specific reagents on activity of rBmGK

Group specific reagents (concentration)	Relative activity (%)
EDTA (1 mM)	0
BME (5 mM)	100
DTT (5 mM)	100
NEM (1 mM)	91
pCMB (1 mM)	98
DEPC (5 mM)	95
PMSF (5 mM)	35

Experiments were performed by incubating the reagents in assay buffer for 10 min and assayed for enzyme activity as described in 'Materials and Methods'.

Table 4. Effect of antifilarials and antiparasitic compounds on activity of rBmGK

Antifilarial and antiparasitic compounds (concentration)	Inhibition (%)
None	0
DEC (5.0 mM)	62·0
Ivermectin (5·0 mM)	50·0
Levamisole (5·0 mM)	65·0
Suramin (10 μM)	82·5
Aurin (50 μM)	83·0

The enzyme was incubated with the listed antifilarials and antiparasitic compounds for 10 min and activity was measured as described in 'Materials and Methods'. Ivermectin was dissolved in DMSO and an equal amount of DMSO was added to control and activity was measured. DMSO showed no inhibitory effect on rBmGK.

straight lines in a double reciprocal plot at different concentrations of GMP and ATP suggested sequential mechanism of reaction for catalysis of BmGK as observed in yeast GK (Li *et al*. 1996). The enzyme follows a ternary complex formation for catalysis. The purified enzyme is highly specific for both phosphate acceptor as well as donor. GMP and ATP were found to be the preferred phosphate acceptor and donor, respectively among different NMPs and NTPs tested. This is in close agreement with most of the known GKs (Oeschger and Bessman, 1966; Kandeel *et al*. 2008). The specificity of BmGK for ATP is a general feature of GKs due to presence of the characteristic structural motif that recognizes an adenine base (Hible *et al*. 2005, 2006*a*). The specificity and affinity of GK for GMP and dGMP differs in different organisms. The efficiency of GK for GMP and dGMP is similar in human erythrocyte, rat liver (Agarwal *et al*. 1978) and calf thymus (Shimono and Sugino, 1971) while for mycobacterium it is only 8%

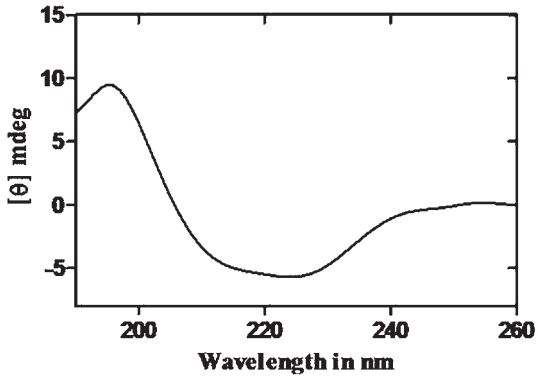

Fig. 6. Far UV CD spectrum of BmGK: Protein spectrum was recorded between 250 and 190 nm wavelength at 25 °C in mdeg on Jasco J810 spectropolarimeter in 1·0 cm pathlength cuvette with 5 μM BmGK. The enzyme consisted of 45% α-helices and 18% β-sheets.

https://doi.org/10.1017/S0031182014000675 Published online by Cambridge University Press

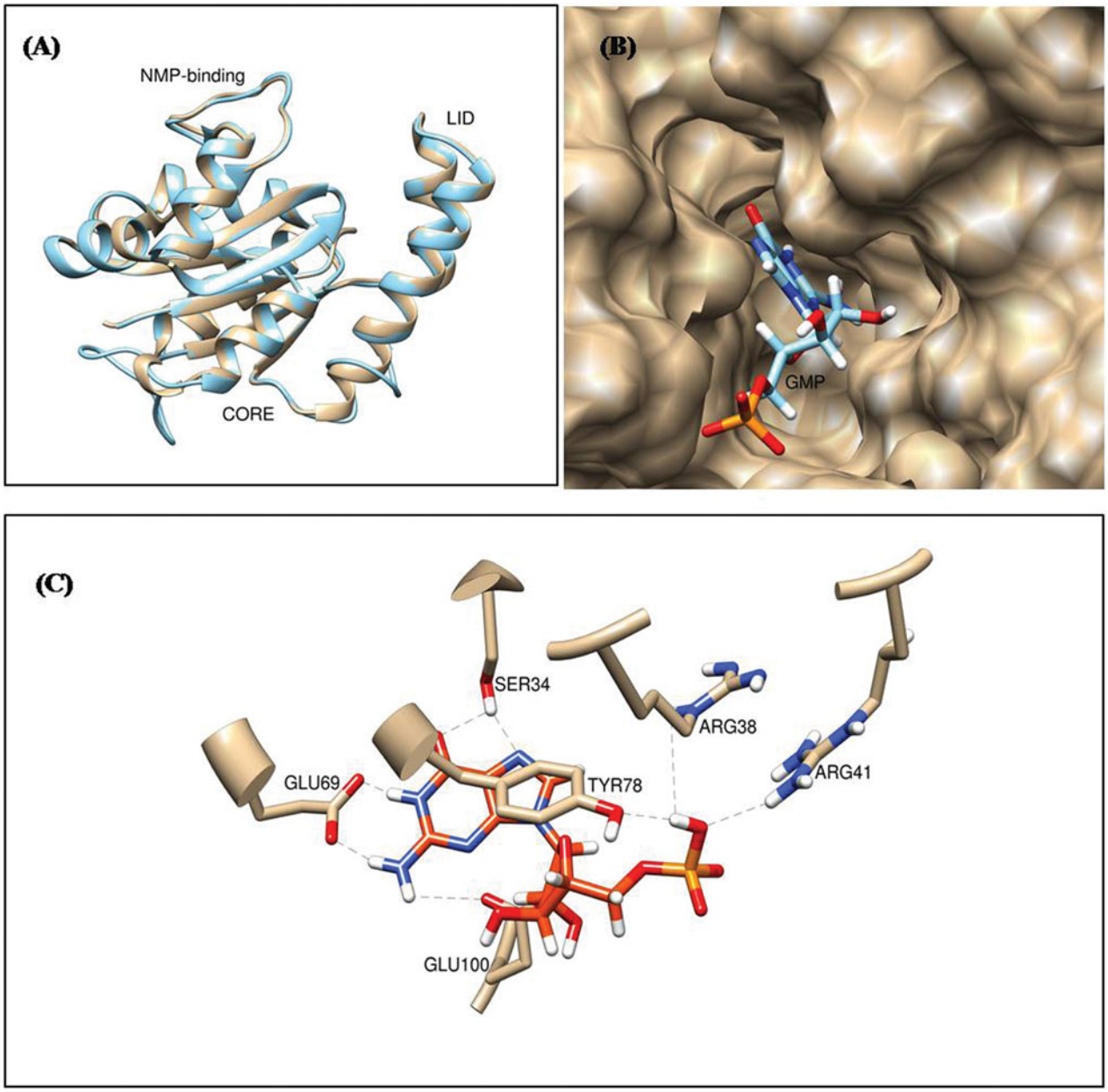

Fig. 7. Homology model of BmGK based on the crystal structure of yeast GK (PDB ID 1EX7). (A) Template yeast and modelled BmGK protein superimposed with RMSD of 0·247 Å for structural comparison; (B) BmGK–GMP complex showing how GMP is accommodated in binding site of BmGK; (C) Hydrogen bonding pattern from docking study of *B. malayi* guanylate kinase with GMP based on superposition (GMP in red-orange; residues involved in H-bonding in brown; and black line represents H-bond).

of GMP for dGMP (Hible *et al*. 2005, 2006*a*). Recombinant BmGK showed 30% catalytic efficiency for dGMP over GMP which is an intermediate between reported efficiencies in yeast (Li *et al*. 1996) and humans (Hible *et al*. 2006*b*).

Effect of different group-specific reagents on BmGK activity suggested that Ser residue seems to play an important role in catalysis. This was supported by the docking study of BmGK with GMP. Lack of inhibition by –SH group specific reagents (NEM and pCMB) and reducing agents, DTT and βME (Buccino and Roth, 1969) indicated an absence of any role of functional –SH groups in catalytic activity of BmGK. The requirement of Mg^{+2} in the catalysis of the reaction is observed since MgATP complex is the true phosphate donor of NMP kinases (Berg *et al*. 2002). EDTA at 1 mM resulted in complete chelation of Mg^{+2} required for catalysis of reaction causing 100% loss of activity. An activation of BmGK catalysis was observed with increasing concentration of free Mg^{+2} (uncomplexed with ATP), a unique property observed in GK. Since concentration of metal ions is known to vary in different localizations in cells owing to different regulatory mechanisms and also Mg^{+2} concentration mediates an association between

https://doi.org/10.1017/S0031182014000675 Published online by Cambridge University Press

Mg^{+2} and ATP/ADP, activation of BmGK by free Mg^{+2} suggest a regulatory role of Mg^{+2} in BmGK catalysis as observed in adenylate kinase of *E. coli* (Tan *et al*. 2009). Similarly, the regulatory role of GTP was also observed in BmGK catalysis which may be due to an endproduct inhibition often observed in regulation of metabolic pathways (Mikkelsen *et al*. 2003). Since the fluorescence behaviour of a tryptophan residue in a protein mirrors its microenvironment in the native state, the observed decrease in the intrinsic fluorescence intensity of BmGK could be the result of various intra-molecular changes in BmGK consequent to its interaction with GTP.

Since GK is a nucleotide synthesizing enzyme essential for organisms, its inhibition would affect parasite growth and survival. Among the different antifilarial and antiparasitic compound tested, DEC, ivermectin and levamisole showed >50% inhibition at higher concentrations. Suramin inhibited 82% activity at 10 μM concentration. Since suramin is known to block G protein-mediated signalling of various GPCR proteins (Chung and Kermode, 2005), inhibition of BmGK with suramin points towards the role of BmGK in signal transduction as reported for GKs (Konrad, 1992). Also, the ability of suramin to inactivate growth factors and enzymes critical to cellular homoeostasis and proliferation (Stein *et al*. 1989) further emphasizes the essential role of GK in *B. malayi*. Since a phosphorylated derivative of GK is involved in nucleotide as well as polypeptide biosynthesis (Oeschger and Bessman, 1966), inhibition of BmGK by aurin can be explained with known function of aurin to inhibit protein biosynthesis and activity of many enzymes involved in cellular metabolism (Okada and Koizumi, 1995). Expression of BmGK in major life stages of *B. malayi* as revealed by western immunoblotting with antiserum raised in rabbit suggests an important role of the enzyme in the development of parasites as anticipated from a housekeeping enzyme involved in nucleotide synthesis.

To better understand the biochemical and kinetic properties of BmGK, its 3D structure was generated based on sequence similarities of well-characterized organisms. Sequence alignment of BmGK showed high sequence similarity with humans, yeast, *E. coli* and *P. falciparum*. Molecular modelling allowed determination of structure and residues involved in substrate binding. Although residues involved in GMP binding are conserved in *B. malayi*, Asp100 is substituted by Glu100 and still there are several other amino acid substitutions in GMP binding region as observed in multiple sequence alignment data and homology modelling. CD analysis and modelling study suggested BmGK to be a typical α/β type protein.

In conclusion, *B. malayi* GK has been overexpressed, purified and characterized. We have reported for the first time the dimeric oligomerization of a guanylate kinase (BmGK) which is unique in eukaryotes studied to date. Similarly, regulatory control on BmGK by GTP as endproduct inhibitor and activation by increasing free Mg is unique to BmGK. The enzyme utilized GMP and ATP, as the preferred phosphate acceptor and donor, respectively. GMP could be replaced with dGMP but with only 30% efficiency. BmGK showed higher catalytic efficiency as compared with human GK and followed ternary complex formation with sequential mechanism of catalysis. Inhibitor binding at protein interfaces is emerging as an attractive strategy for drug discovery (Gokhale *et al*. 1999) and different oligomeric status of GK between *B. malayi* and human have provided evidence for developing parasite-specific inhibitors. Further study of inter-subunit interactions may be fruitful to gain an insight into dimeric structure of BmGK. Thus, structural differences together with different kinetic properties can provide a way to design inhibitors specific to parasite enzyme.

SUPPLEMENTARY MATERIAL

To view supplementary material for this article, please visit http://dx.doi.org/S0031182014000675.

ACKNOWLEDGEMENTS

We gratefully acknowledge the Council of Scientific and Industrial Research (CSIR), New Delhi, for offering a Senior Research fellowship to Smita Gupta to carry out this work. We would like to extend our gratitude to Dr T. K. Chakraborty, Director, CDRI for his invaluable support. CDRI communication number 8639.

REFERENCES

Agarwal, K., Miech, R. and Parks, R. (1978). Guanylate kinases from human erythrocytes, hog brain, and rat liver. *Methods in Enzymology* **51**, 483–490.

Andrade, M., Chacon, P., Merelo, J. and Moran, F. (1993). Evaluation of secondary structure of proteins from UV circular dichroism spectra using an unsupervised learning neural network. *Protein Engineering* **6**, 383–390.

Auvynet, C., Topalis, D., Caillat, C., Munier Lehmann, H., Seclaman, E., Balzarini, J., Agrofoglio, L. A., Kaminski, P. A., Meyer, P. and Deville Bonne, D. (2009). Phosphorylation of dGMP analogs by vaccinia virus TMP kinase and human GMP kinase. *Biochemical and Biophysical Research Communications* **388**, 6–11.

Berg, J. M., Tymoczko, J. L. and Stryer, L. (2002). *Biochemistry*, 5th Edn. W.H. Freeman, New York, NY, USA.

Bockarie, M. J. and Deb, R. M. (2010). Elimination of lymphatic filariasis: do we have the drugs to complete the job? *Current Opinion in Infectious Diseases* **23**, 617–620.

Bradford, M. M. (1976). A rapid and sensitive method for the quantification of microgram quantities of protein utilizing the principle of protein dye binding. *Analytical Biochemistry* **72**, 248–254.

Brady, W. A., Kokoris, M. S., Fitzgibbon, M. and Black, M. E. (1996). Cloning, characterization, and modeling of mouse and human guanylate kinases. *Journal of Biological Chemistry* **271**, 16734–16740.

Buccino, R. J. and Roth, J. S. (1969). Partial purification and properties of ATP: GMP phosphotransferase from rat liver. *Archives of Biochemistry and Biophysics* **132**, 49–61.

Chung, W. C. and Kermode, J. C. (2005). Suramin disrupts receptor-G protein coupling by blocking association of G protein α and $\beta\gamma$ subunits. *Journal of Pharmacology and Experimental Therapeutics* **313**, 191–198.

Crompton, D. W. T. (2010). *First WHO Report on Neglected Tropical Diseases: Working to Overcome the Global Impact of Neglected Tropical Diseases*. World Health Organization, Geneva, Switzerland.

Eftimie, A., Toma, F., Costache, A. Z. and Bucurenci, N. (2007). Characterization of guanylate kinase from gram positive and gram negative microorganisms; preliminary results. *Roumanian Archives of Microbiology and Immunology* **66**, 22.

Fidock, D. A., Rosenthal, P. J., Croft, S. L., Brun, R. and Nwaka, S. (2004). Antimalarial drug discovery: efficacy models for compound screening. *Nature Reviews Drug Discovery* **3**, 509–520.

Gentry, D., Bengra, C., Ikehara, K. and Cashel, M. (1993). Guanylate kinase of *Escherichia coli* K-12. *Journal of Biological Chemistry* **268**, 14316–14321.

Gokhale, R. S., Soumya, S., Balaram, H. and Balaram, P. (1999). Unfolding of *Plasmodium falciparum* triosephosphate isomerase in urea and guanidinium chloride: evidence for a novel disulfide exchange reaction in a covalently cross-linked mutant. *Biochemistry* **38**, 423–431.

Hible, G., Renault, L., Schaeffer, F., Christova, P., Zoe Radulescu, A., Evrin, C., Gilles, A. M. and Cherfils, J. (2005). Calorimetric and crystallographic analysis of the oligomeric structure of *Escherichia coli* GMP kinase. *Journal of Molecular Biology* **352**, 1044–1059.

Hible, G., Christova, P., Renault, L., Seclaman, E., Thompson, A., Girard, E., Munier Lehmann, H. and Cherfils, J. (2006*a*). Unique GMP binding site in *Mycobacterium tuberculosis* guanosine monophosphate kinase. *Proteins: Structure, Function, and Bioinformatics* **62**, 489–500.

Hible, G., Daalova, P., Gilles, A. M. and Cherfils, J. (2006*b*). Crystal structures of GMP kinase in complex with ganciclovir monophosphate and Ap_5G. *Biochimie* **88**, 1157–1164.

Jain, A. N. (2003). Surflex: fully automatic flexible molecular docking using a molecular similarity-based search engine. *Journal of Medicinal Chemistry* **46**, 499–511.

Kandeel, M. and Kitade, Y. (2011). Binding dynamics and energetic insight into the molecular forces driving nucleotide binding by guanylate kinase. *Journal of Molecular Recognition* **24**, 322–332.

Kandeel, M., Nakanishi, M., Ando, T., Shazly, K., Yosef, T., Ueno, Y. and Kitade, Y. (2008). Molecular cloning, expression, characterization and mutation of *Plasmodium falciparum* guanylate kinase. *Molecular and Biochemical Parasitology* **159**, 130–133.

Konrad, M. (1992). Cloning and expression of the essential gene for guanylate kinase from yeast. *Journal of Biological Chemistry* **267**, 25652–25655.

Kumar, V., Spangenberg, O. and Konrad, M. (2001). Cloning of the guanylate kinase homologues AGK1 and AGK2 from *Arabidopsis thaliana* and characterization of AGK1. *European Journal of Biochemistry* **267**, 606–615.

Laemmli, U. K. (1970). Cleavage of structural proteins during the assembly of the head of bacteriophage T4. *Nature* **227**, 680–685.

Li, Y., Zhang, Y. and Yan, H. (1996). Kinetic and thermodynamic characterizations of yeast guanylate kinase. *Journal of Biological Chemistry* **271**, 28038–28044.

Maenpuen, S., Sopitthummakhun, K., Yuthavong, Y., Chaiyen, P. and Leartsakulpanich, U. (2009). Characterization of *Plasmodium falciparum* serine hydroxymethyltransferase – A potential antimalarial target. *Molecular and Biochemical Parasitology* **168**, 63–73.

Mikkelsen, N. E., Johansson, K., Karlsson, A., Knecht, W., Andersen, G., Piskur, J., Munch Petersen, B. and Eklund, H. (2003). Structural basis for feedback inhibition of the deoxyribonucleoside salvage pathway: studies of the *Drosophila* deoxyribonucleoside kinase. *Biochemistry* **42**, 5706–5712.

Miller, W. and Miller, R. (1980). Phosphorylation of acyclovir (acycloguanosine) monophosphate by GMP kinase. *Journal of Biological Chemistry* **255**, 7204–7207.

Oeschger, M. P. and Bessman, M. J. (1966). Purification and properties of guanylate kinase from *Escherichia coli*. *Journal of Biological Chemistry* **241**, 5452–5460.

Okada, N. and Koizumi, S. (1995). A neuroprotective compound, aurin tricarboxylic acid, stimulates the tyrosine phosphorylation cascade in PC12 cells. *Journal of Biological Chemistry* **270**, 16464–16469.

Sali, A. and Blundell, T. L. (1993). Comparative protein modelling by satisfaction of spatial restraints. *Journal of Molecular Biology* **234**, 779–815.

Sambrook, J., Fritsch, E. F. and Maniatis, T. (1989). *Molecular Cloning: A Laboratory Manual*, 2nd Edn. Cold Spring Harbor Laboratory Press, Cold Spring Harbor, NY, USA.

Sekulic, N., Shuvalova, L., Spangenberg, O., Konrad, M. and Lavie, A. (2002). Structural characterization of the closed conformation of mouse guanylate kinase. *Journal of Biological Chemistry* **277**, 30236–30243.

Shimono, H. and Sugino, Y. (1971). Metabolism of deoxyribonucleotides. *European Journal of Biochemistry* **19**, 256–263.

Singh, A. R., Joshi, S., Arya, R., Kayastha, A. M., Srivastava, K. K., Tripathi, L. M. and Saxena, J. K. (2008). Molecular cloning and characterization of *Brugia malayi* hexokinase. *Parasitology International* **57**, 354–361.

Stein, C., LaRocca, R., Thomas, R., McAtee, N. and Myers, C. E. (1989). Suramin: an anticancer drug with a unique mechanism of action. *Journal of Clinical Oncology* **7**, 499–508.

Tan, Y. W., Hanson, J. A. and Yang, H. (2009). Direct Mg^{+2} binding activates adenylate kinase from *Escherichia coli*. *Journal of Biological Chemistry* **284**, 3306–3313.

Vonrhein, C., Schlauderer, G. J. and Schulz, G. E. (1995). Movie of the structural changes during a catalytic cycle of nucleoside monophosphate kinases. *Structure* **3**, 483–490.

Willmon, C., Krabbenhoft, E. and Black, M. (2006). A guanylate kinase/HSV-1 thymidine kinase fusion protein enhances prodrug-mediated cell killing. *Gene Therapy* **13**, 1309–1312.

World Health Organization (2010). *Progress Report 2000–2009 and Strategic Plan 2010–2020 of the Global Programme to Eliminate Lymphatic Filariasis: Halfway Towards Eliminating Lymphatic Filariasis*. World Health Organization, Geneva, Switzerland.

Yan, H. and Tsai, M. D. (1999). Nucleoside monophosphate kinases: structure, mechanism, and substrate specificity. *Advanced Enzymology Related Areas Molecular Biology* **73**, 103–134.

Zhang, Y. L., Zhou, J. M. and Tsou, C. L. (1993). Inactivation precedes conformation change during thermal denaturation of adenylate kinase. *Biochimica et Biophysica Acta (BBA) – Protein Structure and Molecular Enzymology* **1164**, 61–67.